Validation of the MadAnalysis 5 implementation of ATLAS-SUS-13-05

Guillaume Chalons (LPSC Grenoble)

email: chalons@lpsc.in2p3.fr

June 19, 2014

Abstract

In this note we summarise our validation of the ATLAS search for direct third generation in final states with missing transverse momentum and two b-jets in $\sqrt{s} = 8$ TeV [Aad et al.(2013)].

June 19, 2014

1 Description of the implementation of the analysis

The analysis was implemented using the `MadAnalysis5` framework [Conte et al.(2013)Conte, Fuks, and Serret]. To validate the implementation of the analysis we generated 10^5 events for four benchmark points, used in [Aad et al.(2013)] and further refered to:

- **8TeV_b300_n200**: in this scenario the lightest sbottom $\tilde{b}_1$ is the only coloured sparticle contributing to the production process and it only decays via $\tilde{b}_1 \to b\tilde{\chi}_1^0$. The mass of the $(\tilde{b}_1, \tilde{\chi}_1^0)$ pair is $(m_{\tilde{b}_1}, m_{\tilde{\chi}_1^0}) = (300, 200)$ GeV.

- **8TeV_b500_n1**: the scenario is the same as above except that the mass of the $(\tilde{b}_1, \tilde{\chi}_1^0)$ pair is $(m_{\tilde{b}_1}, m_{\tilde{\chi}_1^0}) = (500, 1)$ GeV.

- **8TeV_t250_c155_n150**: in this scenario the only coloured sparticle is the lightest stop $\tilde{t}_1$ and decays exclusively to $\tilde{t}_1 \to b\tilde{\chi}_1^{\pm}$. The subsequent decays of the $\tilde{\chi}_1^{\pm}$ are invisible since the splitting between the $\tilde{\chi}_1^{\pm}$ and the $\tilde{\chi}_1^0$ is small $\Delta m = m_{\tilde{\chi}_1^{\pm}} - m_{\tilde{\chi}_1^0} = 5$ GeV. The mass of the $(\tilde{t}_1, \tilde{\chi}_1^{\pm})$ pair is $(m_{\tilde{t}_1}, m_{\tilde{\chi}_1^{\pm}}) = (250, 155)$ GeV.

- **8TeV_t500_c105_n100**: this scenario is the same as above except that we have $(m_{\tilde{t}_1}, m_{\tilde{\chi}_1^{\pm}}) = (500, 105)$ GeV.

Two sets of SRs, denoted by SRA and SRB, were defined to provide sensitivity to the kinematic topologies associated with the two sets of SUSY mass spectra. SRA targets signal events with large mass splittings between the squark and the neutralino, therefore the benchmark points 8TeV_b500_n1 and 8TeV_t500_c105_n100 are concerned, whereas SRB is designed to enhance the sensitivity when the squark-neutralino mass difference is small, hence benchmark points 8TeV_b300_n200 and 8TeV_t250_c155_n150 are targeted.

The event samples were generated using `MadGraph5_v1.4.8` [Alwall et al.(2011)Alwall, Herquet, Maltoni, Mattelaer, and Stelzer] and passed to `Pythia6` (with the PDF set `CTEQ6L1`) within `MadGraph` through the `pythia-pgs` package. The parameter cards in the form of `slha` files were provided by the `ATLAS` collaboration. We used our own cards for the rest. The x_q^{cut} parameter needed for the merging is defined as $m_{\tilde{q}}/4$ where $m_{\tilde{q}} = m_{\tilde{t}_1}, m_{\tilde{b}_1}$. The generated files in the `StdHep` format were then passed through detector simulation using the modified version of `DELPHES3` [de Favereau et al.(2013)de Favereau, Delaere, Demin, Giammanco, Lematre et al.] as implemented in `MadAnalysis5`. At the level of the detector simulation we used the "medium" selection criteria for electrons [atl()]. The "medium" selection criteria should be the defined as the electrons identification efficiency times the reconstruction and track quality efficiency, however, we set the latter directly to 100% for simplification as it around 97-99%.

All the rest of the detector simulation is set as default as provided in the standard `DELPHES` card for ATLAS. We did not implemented the criteria on the charged p_T fraction (f_{ch}) and on the fraction of the energy contained in the electromagnetic layers of the calorimeter (f_{em}).The number of events was rescaled to a luminosity of 20.1fb^{-1} using the tabulated 8 TeV stops/sbottoms production cross sections with squarks and gluinos decoupled `https://twiki.cern.ch/twiki/bin/view/LHCPhysics/SUSYCrossSections8TeVstopsbottom`.

2 Results and plots

We present in this section the tentative reproduction of the official plots provided in [Aad et al.(2013)]. We first discuss SRA and then SRB.

2.1 Signal Region A (SRA)

The official distributions provided are the M_{CT} distribution (more details can be found in [Tovey(2008), Polesello and Tovey(2010)]) with all selection cuts except the M_{CT} requirement, and the invariant mass of the b-jet pair m_{bb} with all selection cuts except the m_{bb} requirement. The computation of the special kinematic variable M_{CT} was done using the publicly available library which can be downloaded from `http://projects.hepforge.org/mctlib`. The results are displayed in Figure 1.

We now compare our cutflows with the official ones given in Table. 1 and 2. These cutflows have been generated for the following benchmarks

$$SRA : \begin{cases} (m_{\tilde{b}_1}, m_{\tilde{\chi}_1^0}) = (500, 1) \text{ GeV} \\ (m_{\tilde{t}_1}, m_{\tilde{\chi}_1^\pm}, m_{\tilde{\chi}_1^0}) = (500, 120, 100) \text{ GeV} \end{cases} \tag{1}$$

$\tilde{b} \to b\tilde{\chi}_1^0$ (500/1) cutflow for SR SRA, High ΔM, $E_T^{\mathrm{miss}} > 150$ GeV				
cut	# events (scaled to σ and $\mathcal{L}$)	relative change	# events (official)	relative change (official)
Initial number of events	1737.4	1737.4	1738	1738
$E_T^{\mathrm{miss}} > 80$ GeV filter	1628.2	-6.3%	1606.0	-7.6%
Lepton veto	1223.0	-24.9%	1505.0	-6.3%
$E_T^{\mathrm{miss}} > 150$ GeV	1055.4	-13.7%	1323.0	-12.1%
Jet Selection	137.5	-87.0%	119.0	-91.0%
$M_{bb} > 200$ GeV	111.1	-19.2%	96.0	-19.3%
$M_{CT} > 150$ GeV	95.3	-14.2%	82.0	-14.6%
$M_{CT} > 200$ GeV	77.0	-19.2%	67.0	-18.3%
$M_{CT} > 250$ GeV	57.3	-25.6%	51.0	-23.9%
$M_{CT} > 300$ GeV	38.4	-33.0%	35.0	-31.4%

Table 1: Cutflow for the benchmark point $\tilde{b} \to b\tilde{\chi}_1^0$ (500/1) in the Signal Region SRA, High ΔM, $E_T^{\mathrm{miss}} > 150$ GeV.

$\tilde{t} \to b\tilde{\chi}_1^\pm$ (500/120/100) cutflow for SR SRA, High ΔM, $E_T^{\mathrm{miss}} > 150$ GeV				
cut	# events (scaled to σ and $\mathcal{L}$)	relative change	# events (official)	relative change (official)
Initial number of events	1737.4	1737.4	1738	1738
$E_T^{\mathrm{miss}} > 80$ GeV filter	1585.2	-8.8%	1632.0	-6.1%
Lepton veto	862.0	-45.6%	1061.0	-35.0%
$E_T^{\mathrm{miss}} > 150$ GeV	697.5	-19.1%	859.0	-19.0%
Jet Selection	46.5	-93.3%	39	-95.5%
$M_{bb} > 200$ GeV	37.5	-19.4%	32.0	-18.0%
$M_{CT} > 150$ GeV	30.5	-18.7%	26.8	-16.2%
$M_{CT} > 200$ GeV	23.3	-23.6%	20.2	-24.6%
$M_{CT} > 250$ GeV	16.5	-29.2%	13.2	-34.7%
$M_{CT} > 300$ GeV	9.2	-44.2%	7.7	-41.7%

Table 2: Cutflow for the benchmark point $\tilde{t} \to b\tilde{\chi}_1^\pm$ (500/120/100) in the Signal Region SRA, High ΔM, $E_T^{\mathrm{miss}} > 150$ GeV.
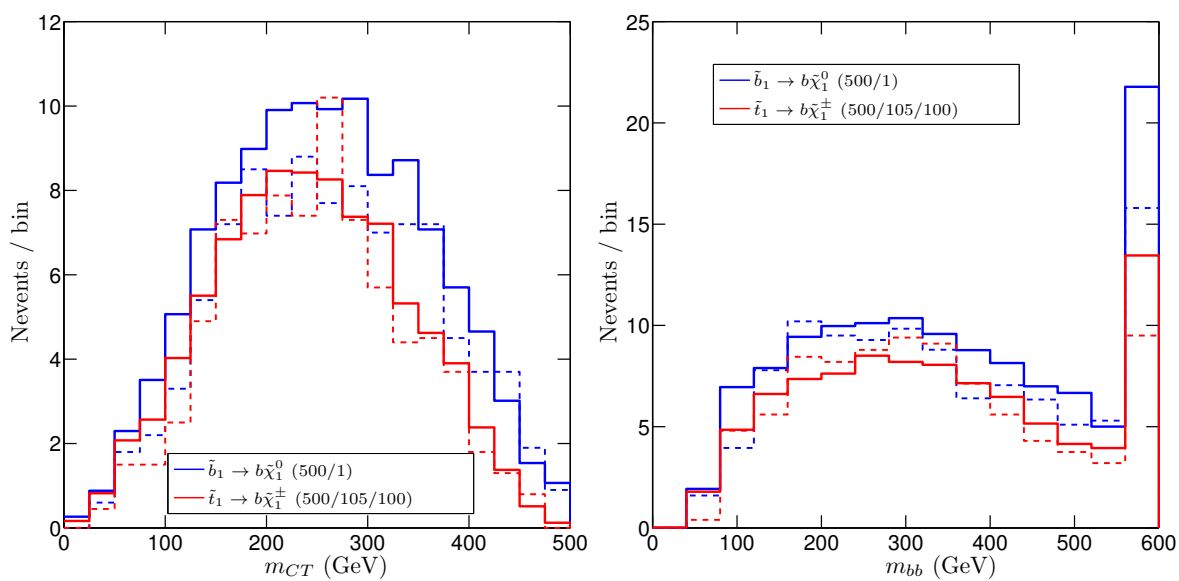
Figure 1: *Left*: M_{CT} distribution (in GeV) in SRA with all selection cuts except the M_{CT} requirement. *Right*: m_{bb} distribution (in GeV) with all selection cuts except the m_{bb} threshold. The solid line is the official plot and the dashed-dotted line is our own reimplementation. The rightmost bins in the figures include the overflows.

3   Signal Region B (SRB)

The official distributions provided are the $H_{T,3}$ and E_T^{miss} distributions. $H_{T,3}$ is defined as the scalar sum of the p_T of the n jets, without including the three leading jets. The official plots display the $H_{T,3}$ and E_T^{miss} distributions without their respective threshold. Using our own implementation the resulting plots are displayed in Figure 2. For this signal region there are discrepancies between the official analysis and our reimplementation. For the $H_{T,3}$ distribution (left panel of Figure 2), the region of interest will be the one where $H_{T,3} < 50$ GeV, where we have the largest discrepancies, where our implementation is in excess with respect to the official one. The second bin is empty since reconstructed jets are required to have $p_T > 20$ GeV (there is a 10 GeV binning). For the E_T^{miss} (right panel of Figure 2) our implementation also predicts an excess of events with respect to the official one, especially in the first bin of the left panel of Fig. 2). It seems that we have too many events with only three jets. However the agreement seems to be better for the 8TeV_b300_n200 benchmark point in the E_T^{miss} distribution and the largest discrepancies are found in the 8TeV_t250_c155_n150 scenario. We now turn on the comparison with the official cutflows given in Table. 3 and Table. 4. These cutflows have been generated for the following benchmarks

$$SRB : \begin{cases} (m_{\tilde{b}_1}, m_{\tilde{\chi}_1^0}) = (350, 320) \text{ GeV} \\ (m_{\tilde{t}_1}, m_{\tilde{\chi}_1^\pm}, m_{\tilde{\chi}_1^0}) = (500, 420, 400) \text{ GeV} \end{cases} \quad (2)$$

cut	$\tilde{b} \to b\tilde{\chi}_1^0$ (350/320) cutflow for SR SRB, Low ΔM, $\text{E}_\text{T}^{\text{miss}} > 250$ GeV			
	# events (scaled to σ and $\mathcal{L}$)	relative change	# events (official)	relative change (official)
Initial number of events	16388.7	16388.7	16241	16241
$E_T^{\text{miss}} > 80$ GeV filter	5963.7	-63.6%	6221.0	-61.7%
Lepton veto	4450.4	-25.4%	4069.0	-34.6%
$E_T^{\text{miss}} > 250$ GeV	724.5	-83.7%	757.0	-81.4%
Jet Selection	6.6	-99.1%	7.9	-99.0%
$H_{T,3} < 50$ GeV	5.8	-12.1%	5.2	-34.2%

Table 3:   Cutflow for the benchmark point $\tilde{b} \to b\tilde{\chi}_1^0$ (350/320) in the Signal Region SRB, Low ΔM, $\text{E}_\text{T}^{\text{miss}} > 250$ GeV.

$\tilde{t} \to b\tilde{\chi}_1^\pm$ (500/420/400) cutflow for SR SRB, Low ΔM, $E_T^{\text{miss}} > 250$ GeV				
cut	# events (scaled to σ and $\mathcal{L}$)	relative change	# events (official)	relative change (official)
Initial number of events	1737.4	1737.4	1738	1738
$E_T^{\text{miss}} > 80$ GeV filter	1117.9	-35.7%	1329.0	-23.5%
Lepton veto	709.2	-36.6%	669.0	-49.7%
$E_T^{\text{miss}} > 250$ GeV	91.5	-87.1%	93.0	-86.1%
Jet Selection	6.2	-93.2%	6.2	-93.3%
$H_{T,3} < 50$ GeV	4.5	-27.4%	3.0	-51.6%

Table 4: Cutflow for the benchmark point $\tilde{t} \to b\tilde{\chi}_1^\pm$ (500/420/400) in the Signal Region SRB, Low ΔM, $E_T^{\text{miss}} > 250$ GeV.
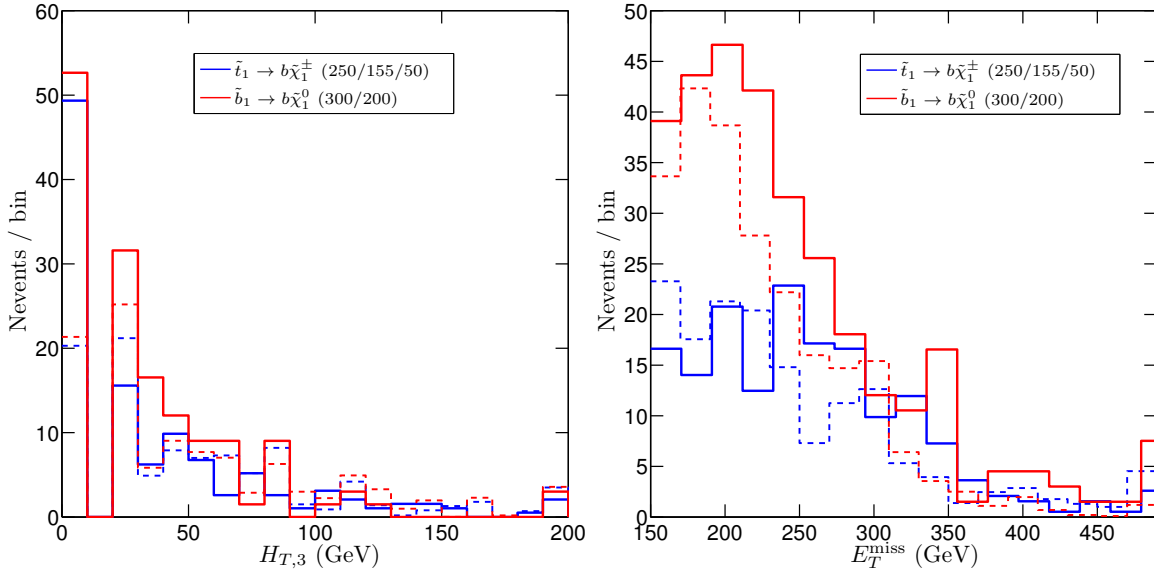

Figure 2: *Left*: $H_{T,3}$ distribution (in GeV) in SRB with all selection cuts except the $H_{T,3}$ requirement. *Right*: E_T^{miss} distribution (in GeV) with all selection cuts except the E_T^{miss} threshold. The solid line is the official plot and the dashed-dotted line is our own reimplementation. The rightmost bins in the figures include the overflows.

References

[Aad et al.(2013)] G. Aad et al. (ATLAS), JHEP **1310**, 189 (2013), `1308.2631`.

[Conte et al.(2013)Conte, Fuks, and Serret] E. Conte, B. Fuks, and G. Serret, Comput.Phys.Commun. **184**, 222 (2013), `1206.1599`.

[Alwall et al.(2011)Alwall, Herquet, Maltoni, Mattelaer, and Stelzer] J. Alwall, M. Herquet, F. Maltoni, O. Mattelaer, and T. Stelzer, JHEP **1106**, 128 (2011), `1106.0522`.

[de Favereau et al.(2013)de Favereau, Delaere, Demin, Giammanco, Lematre et al.] J. de Favereau, C. Delaere, P. Demin, A. Giammanco, V. Lematre, et al. (2013), `1307.6346`.

[atl()] ATL-COM-PHYS-2013-1287.

[Tovey(2008)] D. R. Tovey, JHEP **0804**, 034 (2008), `0802.2879`.

[Polesello and Tovey(2010)] G. Polesello and D. R. Tovey, JHEP **1003**, 030 (2010), `0910.0174`.